CHAPTER 4

RESULTS

4.1 Characterisation of Specimens

In this study, Stereolithography (SLA), Digital Light Processing (DLP), and Liquid Crystal Display (LCD) were used to fabricate the 3D printing denture base resin to elucidate the effect of different vat polymerization techniques in terms of mechanical, physical, and biological properties.

4.2 Mechanical Properties

4.2.1 Flexural Strength and Modulus

The one-way ANOVA analysis revealed a significant difference in flexural strength across all testing groups ($p < 0.001$). Notably, each group surpassed the minimum requirement of 65 MPa as per the ISO standards (*ISO 20795-1. Dentistry-Base Polymers-Part 1: Denture Base Polymers International Organization for Standardization; 2nd Ed. Geneva, Switzerland. 2013*, 2013). The SLA group exhibited the highest flexural strength, with a mean value of $(150.68 \pm 7.93)\ MPa$, while DLP showed $(133.39 \pm 12.66)\ MPa$, followed closely by LCD at $(133.28 \pm 9.39)\ MPa$. Tukey's post hoc of pairwise comparison indicated a significant difference between the SLA group and both the DLP and LCD groups ($p = 0.002$); however, no statistical differences were observed between the LCD and DLP groups.

Contrarily, the flexural modulus demonstrated no significant differences between all groups ($p = 0.256$). Nevertheless, it is worth noting that all groups exceeded the ISO minimum requirement of 2 GPa. These findings are visually represented in Figure 4.1 and Figure 4.2, providing a clear overview of the observed trends in flexural strength and modulus across the different groups. Detail results of the flexural strength and modulus were tabulated in Table 4.1.

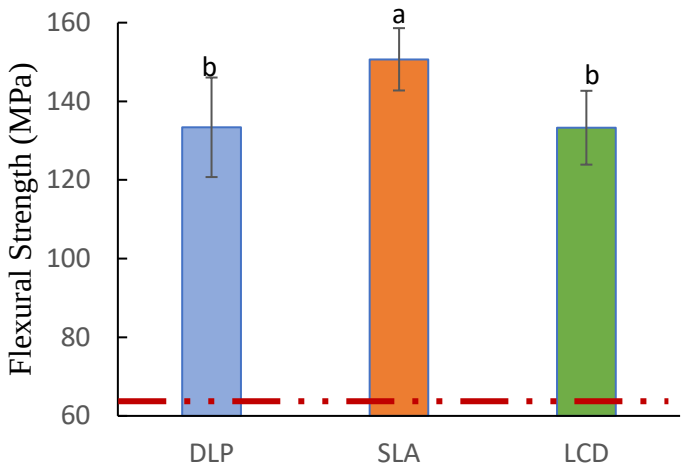

Figure 4.1: Flexural strength of the 3D-printed denture base resin. The red dash-dotted line represents the ISO minimum requirement. Similar letters represent insignificant differences.

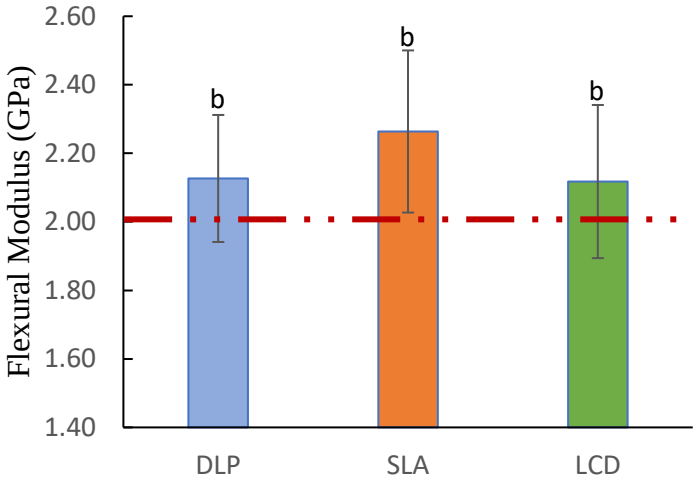

Figure 4.2: Flexural modulus of the 3D-printed denture base resin. The red dash-dotted line represents the ISO minimum requirement. Similar letters represent insignificant differences.

4.2.2 Fracture Toughness

Statistical analysis through one-way ANOVA proved that the fracture toughness of the 3D-printed denture base had significant differences among all testing groups ($p = 0.013$). The fracture toughness of the specimens was in line with the trend observed in flexural strength, the SLA group exhibited the highest fracture toughness across all groups, recording a value of $(1.51 \pm 0.115)\ MPa/m^2$. Conversely, the LCD group demonstrated the lowest fracture toughness, measuring $(1.464 \pm 0.049)\ MPa/m^2$. Tukey's post hoc revealed no significant distinction between the LCD and DLP groups ($p = 0.446$), nor between the DLP and SLA groups ($p = 0.14$). However, the SLA group exhibited a significant difference from the LCD group ($p = 0.01$). It is worth noting that none of the tested groups met the minimum requirements of 1.9 MPa/m^2 as stipulated by ISO recommendations. The results are presented in a graph and illustrated in Figure 4.3. Detail result of the fracture toughness was tabulated in Table 4.1.

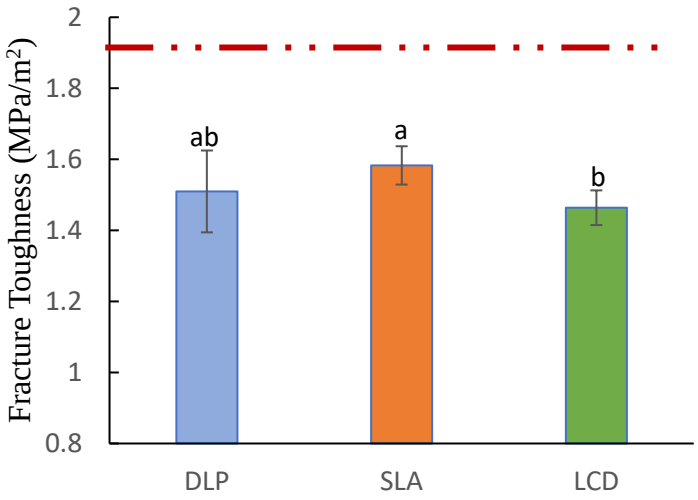

Figure 4.3: Fracture toughness of the 3D-printed denture base resin. The red dash-dotted line represents the ISO minimum requirement. Similar letters represent insignificant differences.

4.2.3 Surface Hardness

Diamond-shaped indentation was observed on the specimen after testing with the Vicker hardness machine (Figure 4.4). One-way ANOVA showed that there is a significant difference among the surface hardness of all groups ($p < 0.001$). Similar to the flexural strength and fracture toughness, the SLA had once again showed the highest surface hardness among all groups $(17.98 \pm 0.83)VH$. Tukey's post hoc of pairwise comparison showed that the SLA group has statistical difference against the DLP ($p = 0.001$) and LCD ($p < 0.001$) group. Additionally, no significant differences were found between the DLP and LCD group ($p = 0.363$). Although the ISO 20795-1 did not outline the acceptable hardness value for the denture base resin, the restoration base resin was expected to have a surface hardness between (15-18) HV (Nair et al., 2022). In this study, all specimens 3D printed with different vat polymerization techniques have an acceptable surface hardness. Figure 4.5 presents the surface hardness results in graphical representation, and Table 4.1 presents the summary of the testing results for the mechanical properties in this study.

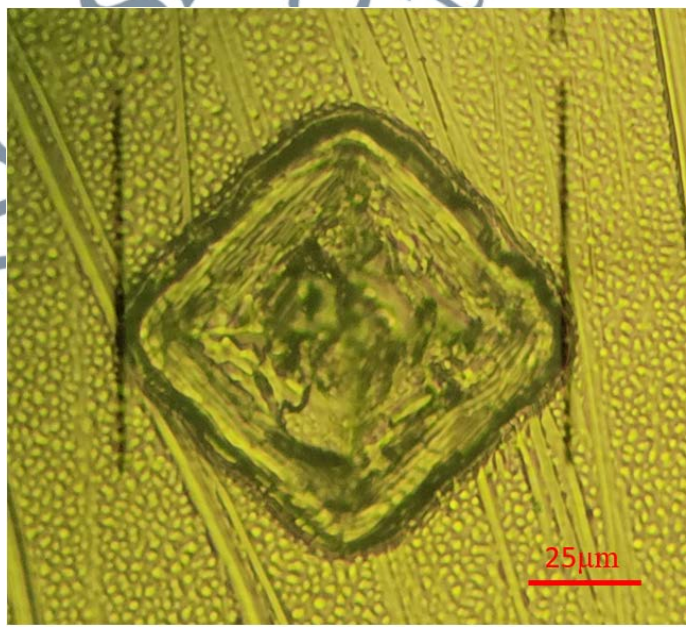

Figure 4.4: Diamond-shaped indentation on the tested specimen

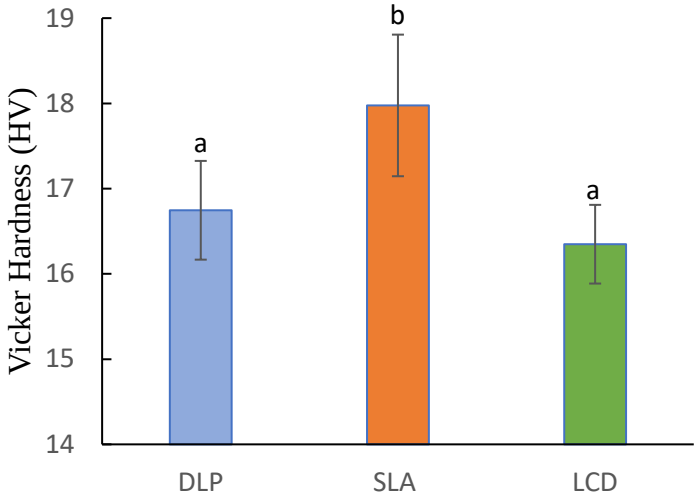

Figure 4.5: Surface hardness of the 3D-printed denture base resin. Similar letters represent insignificant differences.

Table 4.1: Results of the mechanical properties of the 3D-printed denture base

Properties	DLP	SLA	LCD	One-way ANOVA
	Mean ± (SD)	Mean ± (SD)	Mean ± (SD)	F-and P-value
	95% CI [Upper || Lower]	95% CI [Upper || Lower]	95% CI [Upper || Lower]	
Flexural Strength (MPa)	133.39 (12.66)^{b}	150.68 (7.93)^{a}	133.28 (9.39)^{b}	$F = 9.664$
	[142.44||124.34]	[156.35||145.00]	[140.00||126.57]	$p < 0.001^{*}$
Flexural Modulus (GPa)	2.127 (0.186)^{b}	2.264 (0.237)^{b}	2.118 (0.224)^{b}	$F = 1.433$
	[2.259||1.994]	[2.433||2.094]	[2.277||1.958]	$p = 0.256$
Fracture Toughness (MPa/m^2)	1.51(0.115)^{ab}	1.583(0.054)^{a}	1.464(0.049)^{b}	$F = 5.243$
	[1.598||1.421]	[1.624||1.541]	[1.501||1.426]	$p = 0.013^{*}$
Surface Hardness (HV)	16.75(0.58)^{a}	17.98(0.83)^{b}	16.35(0.46)^{a}	$F = 17.449$
	[17.16||16.33]	[18.57||17.38]	[16.68||16.02]	$p < 0.001^{*}$

* Statistically significant was set at 0.05. Statistical difference was represented with different superscripts.

4.3 Physical Properties

4.3.1 Surface Morphology

All specimens that were 3D-printed with different vat polymerization techniques showed similar layering structures on the surface, 45° diagonal line across the specimens' surface. This illustrated the layer-by-layer building mechanism of additive manufacturing. However, the layering structure seemed to be removed after sanding and polishing the specimens to a certain depth as shown in Figure 4.6. This confirmed that the 3D printing's layer-by-layer construction primarily influenced the exterior surface, whereas the main body of the specimens retained a predominantly solid structure with minor voids that might have been caused during the mechanical sanding and polishing. No other differences were observed in surface morphology among all the testing groups before undergoing mechanical sanding and polishing. Consequently, after thorough mechanical sanding and polishing, the surfaces of all the specimens appeared similar.

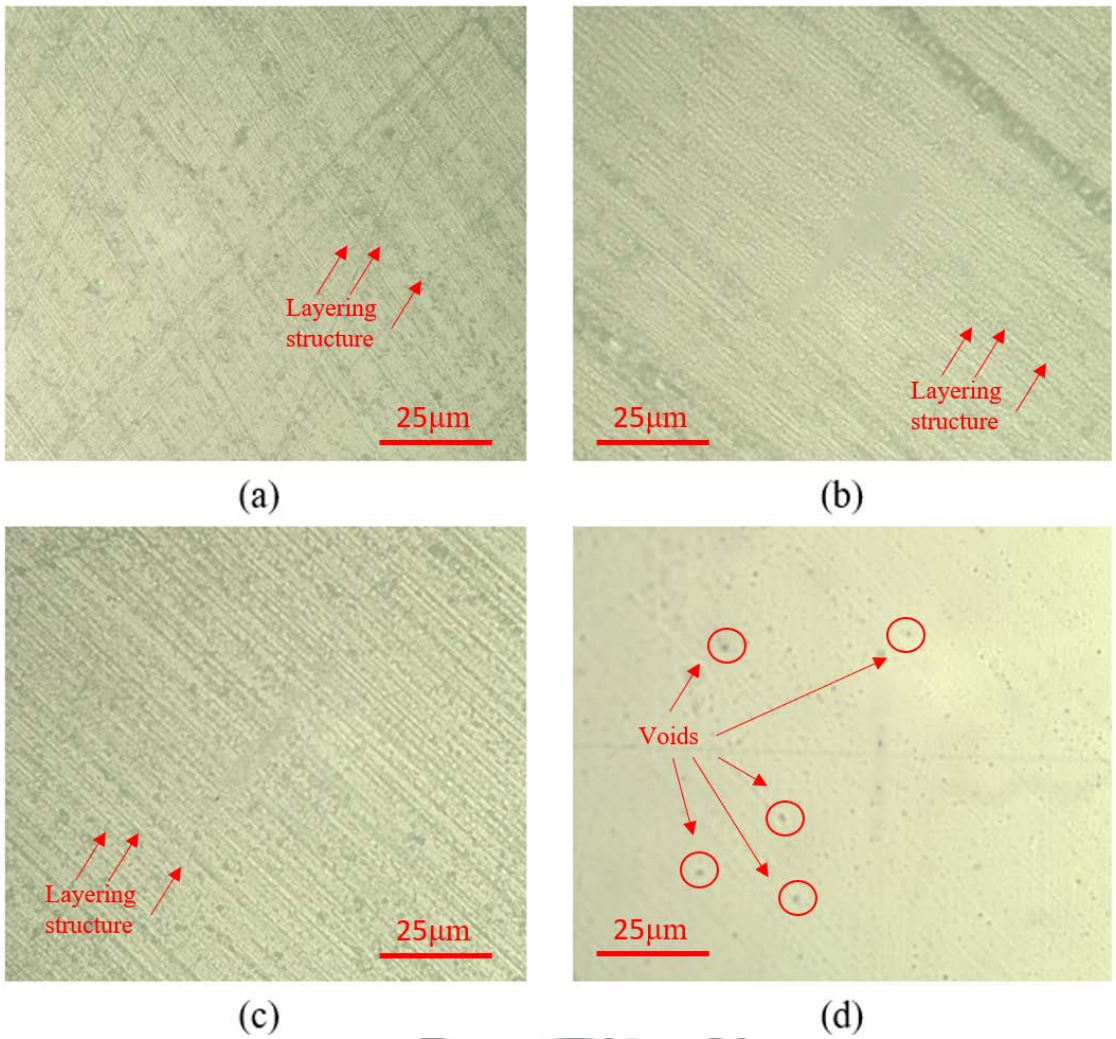

Figure 4.6: Optical microscope image of 3D-printed denture base with different vat polymerization techniques: (a) SLA, (b) DLP, and (c) LCD. (d) Representative surface morphology of all specimens after sanding and polishing.

4.3.2 Water Sorption and Solubility

The water sorption (W_{sp}) for all tested groups had met the ISO standard requirement of 32 $\mu g/mm^3$. However, none of the groups complied with the specified water solubility (W_{sl}) limits, 1.6 $\mu g/mm^3$. One-way ANOVA proved that both water sorption and solubility showed statistically significant differences among all groups ($p < 0.001$). The DLP group exhibited the highest water sorption and solubility values at (31.51 $\pm$ 0.92) $\mu g/mm^3$ and (5.32 $\pm$ 0.61) $\mu g/mm^3$, respectively, which were significantly greater than those of the LCD and SLA groups. Conversely, no significant

differences were observed between the LCD and SLA groups ($p = 0.929$). The SLA group demonstrated the lowest water sorption and solubility values at (27.7 ± 0.4) $\mu g/mm^3$ and (3.03 ± 0.49) $\mu g/mm^3$, respectively. In comparison, the LCD group exhibited slightly higher values at (28.46 ± 0.38)$\mu g/mm^3$ and (3.2 ± 1) $\mu g/mm^3$. The water sorption and solubility results were graphically illustrated in Figure 4.7 and Figure 4.8, and the detailed results were tabulated in Table 4.2.

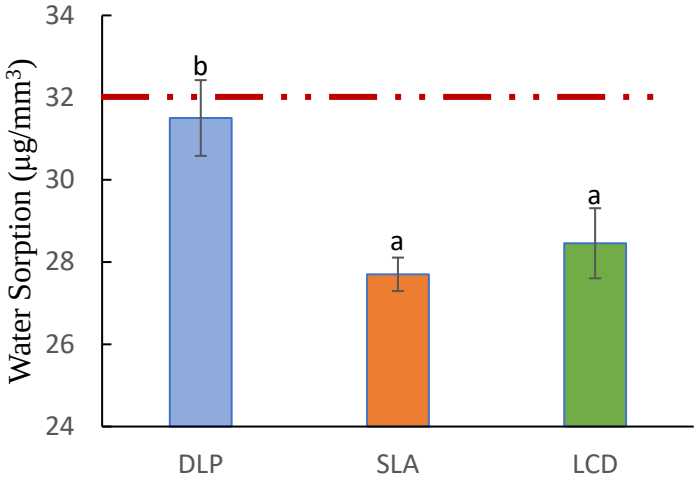

Figure 4.7: Water sorption of the 3D-printed denture base resin. The red dash-dotted line represents the maximum limits in accordance with the ISO. Similar letters represent insignificant differences.

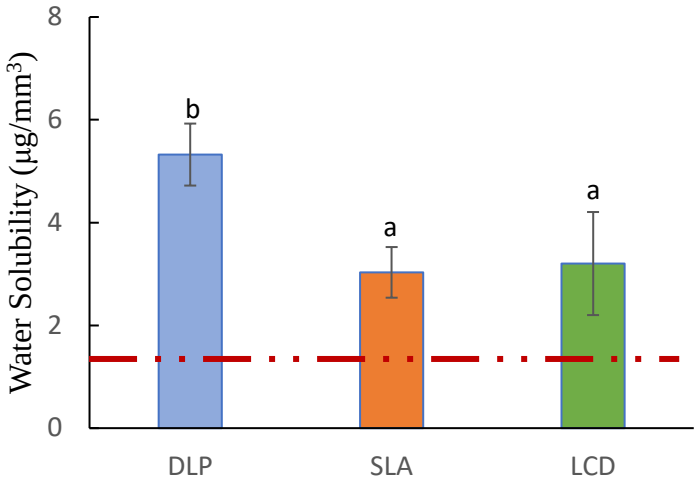

Figure 4.8: Water solubility of the 3D-printed denture base resin. The red dash-dotted line represents the maximum limits in accordance with the ISO. Similar letters represent insignificant differences.

4.3.3 Degree of Conversion

The degree of conversion (DC) was examined through the Fourier Transform Infra-red spectroscopy (FTIR) to determine the effect of different vat polymerization techniques on the 3D-printed denture base. Figure 4.9 shows the FTIR spectrum of the uncured and cured resin. The DC was calculated with the peak observed at the wavenumber of 1637cm^{-1} and 1608cm^{-1}.

The calculated DC for the 3D-printed specimens was $(53.24 \pm 7.77)\%$, $(61.7 \pm 3.42)\%$, and (57.86 ± 4.59) for DLP, SLA, and LCD respectively (Figure 4.10). One-way ANOVA analysis found a significant difference between the tested group ($p = 0.035$). The SLA group exhibited the highest DC and was statistically significant against the DLP group ($p = 0.028$). However, no statistically significant differences were observed between the DLP and LCD groups ($p = 0.292$), as well as between the SLA and LCD groups ($p = 0.418$). The summarized results of the physical properties were tabulated in Table 4.2.

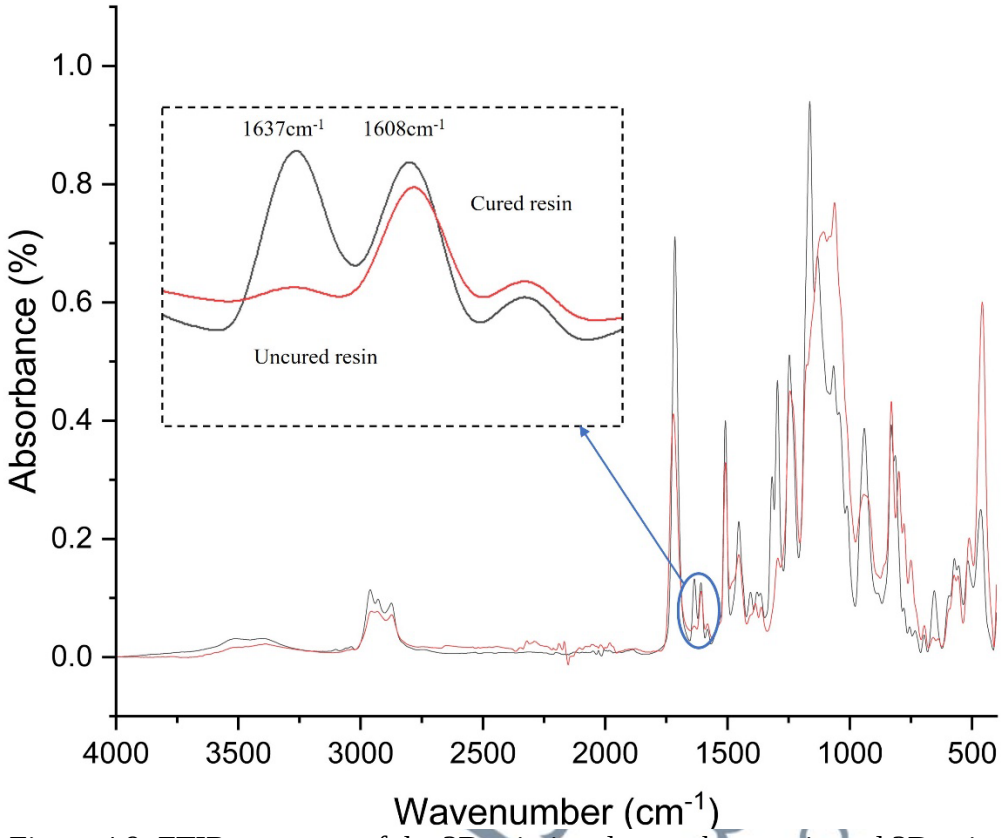

Figure 4.9: FTIR spectrum of the 3D printing denture base resin and 3D-printed denture base specimen

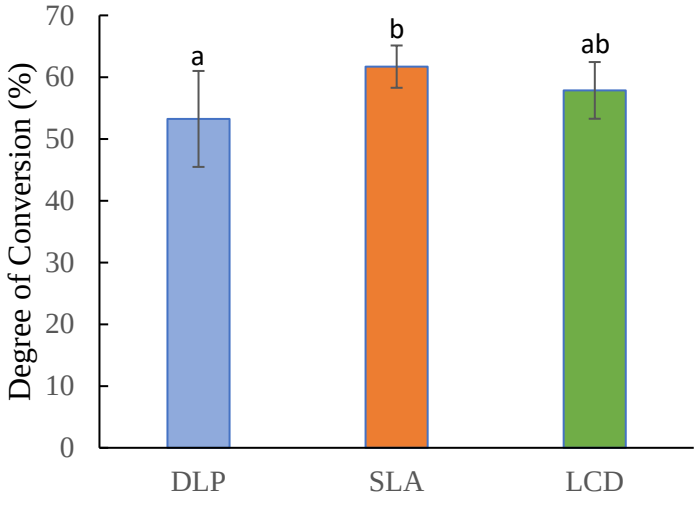

Figure 4.10: Degree of conversion of the 3D-printed denture base resin. Similar letters represent insignificant differences.

Table 4.2: Results of the physical properties of the 3D-printed denture base

Properties	DLP	SLA	LCD	One-way ANOVA
	Mean ± (SD)	Mean ± (SD)	Mean ± (SD)	F-and P-value
	95% CI [Upper || Lower]	95% CI [Upper || Lower]	95% CI [Upper || Lower]	
Water Sorption (μg/mm^3)	31.51 (0.92)^b [32.65||30.36]	27.7 (0.40)^a [28.20||27.20]	28.46 (0.85)^a [29.51||27.40]	$F = 35.021$ $p < 0.001^*$
Water Solubility (μg/mm^3)	5.32 (0.61)^b [6.07||4.57]	3.03 (0.49)^a [3.64||2.42]]	3.2 (1.00)^a [4.45||1.96]	$F = 15.091$ $p < 0.001^*$
Degree of Conversion (%)	53.24(7.77)^a [60.42||46.05]	61.7(3.42)^b [64.87||58.54]	57.86(4.59)^{ab} [62.10||53.61]	$F = 4.053$ $p = 0.035^*$

* Statistically significant was set at 0.05. Statistical difference was represented with different superscripts.

4.4 Biological Properties

4.4.1 Cell Viability

The cytotoxicity of the 3D-printed denture base was characterized through the cell viability of the HGFs. The direct contact method was conducted in this test to determine the cytotoxicity of the 3D-printed denture base more accurately as the specimens were directly in contact with the cultured cells, similar to the oral condition. According to the ISO 10993-5, the cell viability has to be more than 70% to be considered as non-toxic. The cell viability of the tested group was recorded at $(70.06 \pm 5.98)\%$, $(75.99 \pm 6.59)\%$, and $(74.76 \pm 5.47)\%$ for DLP, SLA, and LCD group, respectively. In accordance with the ISO, each of the tested groups exhibited a cell viability exceeding 70%. Figure 4.11 showed the growing condition of the HGFs in the 12-well plate after 48 hours of incubation. This substantiates that the 3D-printed denture base is non-toxic to oral cells, irrespective of the vat polymerization techniques employed for specimen printing. Additionally, one-way ANOVA showed no significant differences between all

groups ($p = 0.141$). The graph of cell viability exhibited by the 3D-printed specimens was illustrated in Figure 4.12.

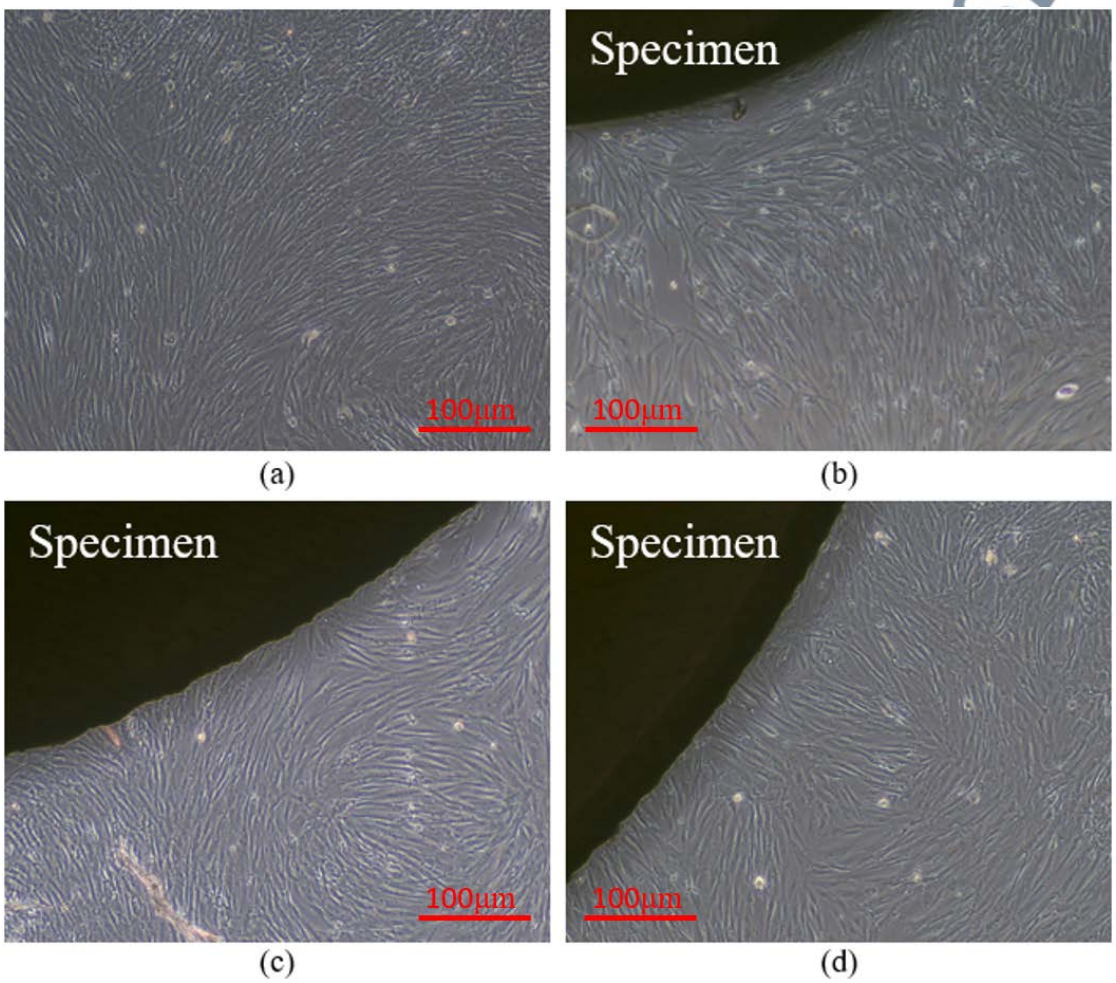

Figure 4.11: Condition of the HGFs after 48 hours of incubation in the 12-well plate. (a) Control well (without specimen treatment), (b) DLP, (c) SLA, and (d) LCD

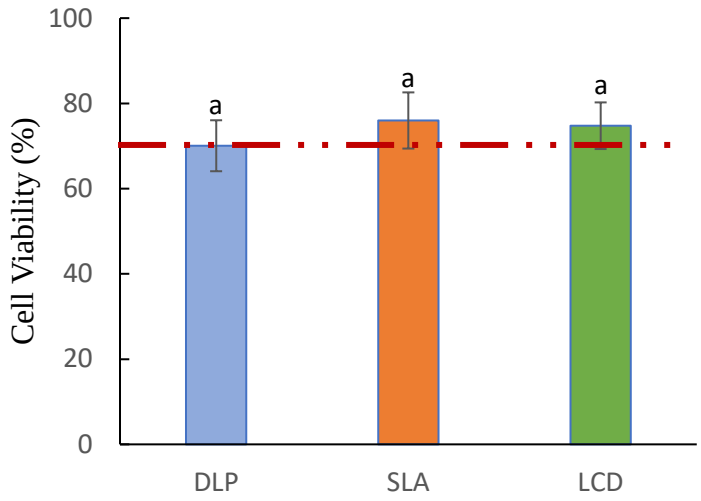

Figure 4.12: Cell viability of the 3D-printed denture base resin. The red dash-dotted line represents the ISO minimum requirement. Similar letters represent insignificant differences.

4.4.2 Fungal Adherence

The adherence assay of *C. albicans* on the 3D-printed dentures was carried out and showed statistically significant difference, as confirmed by one-way ANOVA ($p = 0.029$). Among the tested groups, DLP displayed the least fungal adherence, with the lowest amount of *C. albicans* adhering to the specimen surface (131.61 ± 48.38) CFU/ml. Following this, LCD demonstrated slightly higher adhesion at (167.89 ± 83.1) CFU/ml, while SLA exhibited the highest fungal adhesion (221.94 ± 65.8) CFU/ml. The fluorescent microscopy test had confirmed the findings in the CFU counting test, whereby the most fungal adhesion was found in the SLA group, followed by the LCD and DLP (Figure 4.13). Tukey's post hoc showed no significant differences between the DLP and LCD groups ($p = 0.497$), nor between the SLA and LCD groups ($p = 0.224$). However, significant differences were reported between the DLP and SLA groups ($p = 0.023$). Detailed results of *C. albicans*

adherence on the 3D-printed specimens were graphically illustrated in Figure 4.14. The results of the biological properties were summarized and tabulated in Table 4.3.

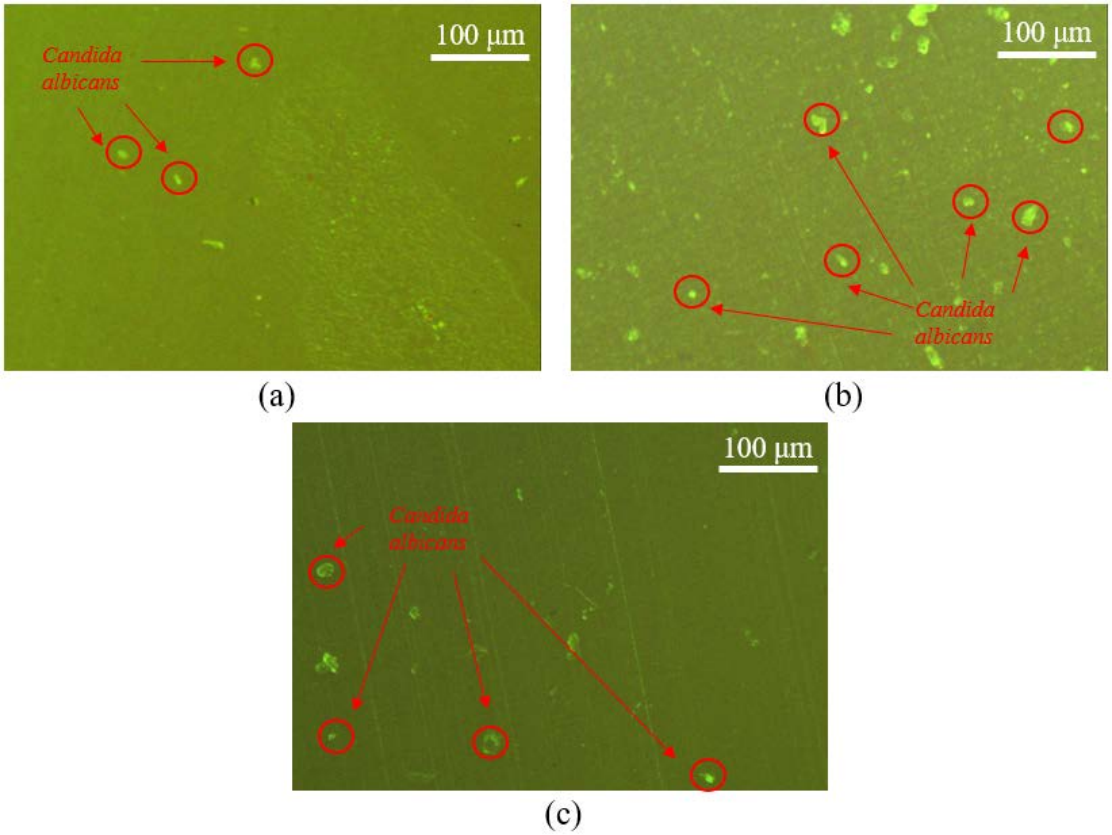

Figure 4.13: Fluorescent microscope image of *C. albicans* adhered on the 3D-printed specimens: (a) DLP, (b) SLA, and (c) LCD

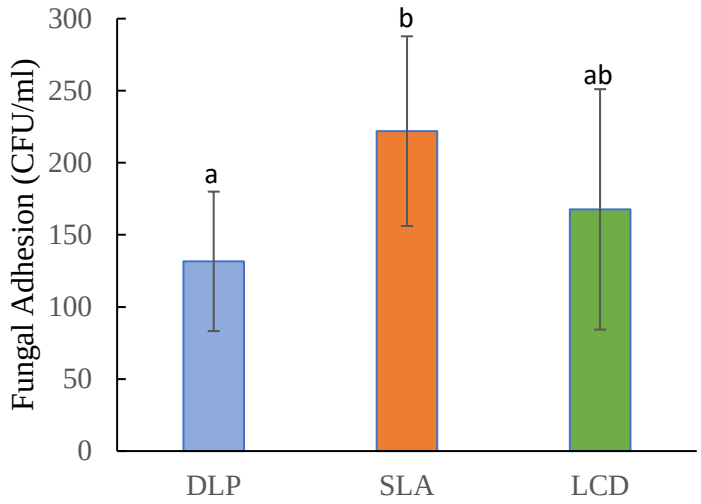

Figure 4.14: Fungal adhesion of the 3D-printed denture base resin. Similar letters represent insignificant differences.

Table 4.3: Results of the biological properties of the 3D-printed denture base

Properties	DLP	SLA	LCD	One-way ANOVA
	Mean ± (SD)	Mean ± (SD)	Mean ± (SD)	
	95% CI [Upper || Lower]	95% CI [Upper || Lower]	95% CI [Upper || Lower]	F-and P-value
Cell Viability (%)	70.06(5.98)[a]	75.99(6.59)[a]	74.76(5.47)[a]	$F = 2.152$
	[75.06||65.06]	[79.34||70.19]	[81.50||70.48]	$p < 0.141$
Microbial Adhesion (CFU/ml)	131.61 (48.38)[a]	221.94 (65.80)[b]	167.89 (83.10)[ab]	$F = 4.109$
	[168.8||94.43]	[272.5||171.4]	[231.8||104.0]	$p < 0.029^{*}$
Fluorescent Microscope	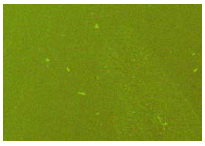	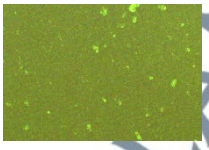	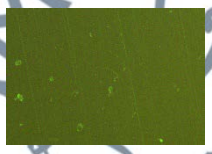	

* Statistically significant was set at 0.05. Statistical difference was represented with different superscripts.